



# Platinum nanoparticle-decorated carbon nanotube clusters on screen-printed gold nanofilm electrode for enhanced electrocatalytic reduction of hydrogen peroxide

Xiangheng Niu<sup>a</sup>, Hongli Zhao<sup>a</sup>, Chen Chen<sup>a</sup>, Minbo Lan<sup>a,b,\*</sup>

<sup>a</sup> Shanghai Key Laboratory of Functional Materials Chemistry, and Research Centre of Analysis and Test, East China University of Science and Technology, Shanghai 200237, PR China

<sup>b</sup> State Key Laboratory of Bioreactor Engineering, East China University of Science and Technology, Shanghai 200237, PR China

## ARTICLE INFO

### Article history:

Received 4 November 2011

Received in revised form 4 January 2012

Accepted 6 January 2012

Available online 15 January 2012

### Keywords:

Platinum nanoparticle

Multi-walled carbon nanotube cluster

Screen-printed gold nanofilm electrode

Electrocatalytic reduction

Hydrogen peroxide

## ABSTRACT

In the present study the electrocatalytic behavior of platinum nanoparticle-decorated multi-walled carbon nanotube clusters vertically aligned on a screen-printed gold nanofilm electrode substrate (SPGFE/MWCNTC/PtNP) toward hydrogen peroxide was intensively investigated. Oriented multi-walled carbon nanotube clusters (MWCNTC) were firstly well-organized onto the screen-printed gold film electrode (SPGFE) surface by covalent immobilization, and then platinum nanoparticles (PtNPs) dispersed on the MWCNTC structure were in situ synthesized by electrochemically reducing chloroplatinic acid. It was demonstrated that the MWCNTC/PtNP hybrid structure on the SPGFE substrate could significantly enhance the electrochemical reduction of hydrogen peroxide in neutral solutions. Compared with platinum nanoparticles loading on disordered multi-walled carbon nanotubes (SPGFE/MWCNT/PtNP), the proposed SPGFE/MWCNTC/PtNP exhibited more sensitive responses for hydrogen peroxide reduction. The fabricated electrode provided linear current responses for hydrogen peroxide in the concentration range from 5 to 2000  $\mu\text{M}$  with a detection limit of 1.23  $\mu\text{M}$ . The non-enzymatic sensor also offered good reproducibility and high selectivity for hydrogen peroxide detection. The carbon nanotube cluster/platinum nanoparticle hybrid system holds great promise as a scaffold to fabricate enzyme biosensors.

© 2012 Elsevier Ltd. All rights reserved.

## 1. Introduction

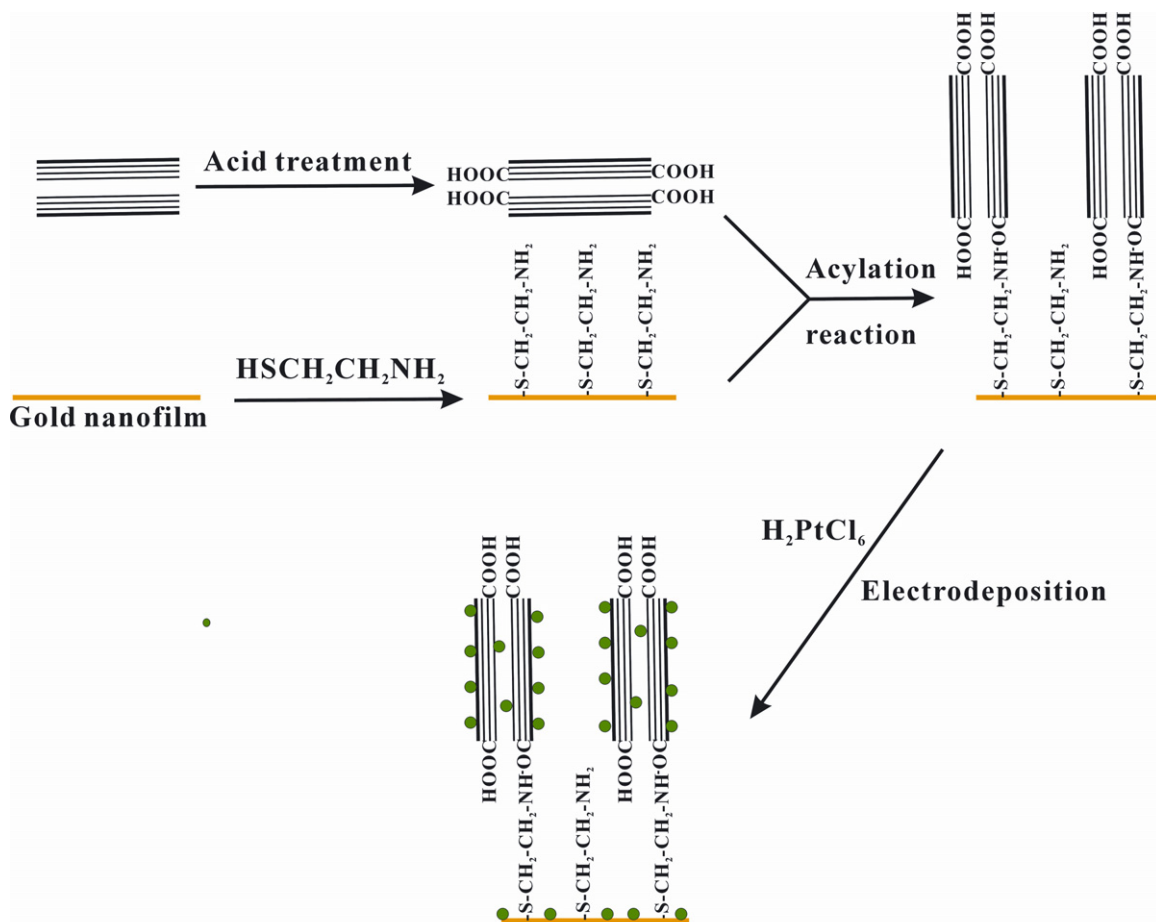
Since the early 1990s, carbon nanotubes (CNTs) have always been attracting growing attention because of their unique properties such as one-dimensional nature, high conductivity, structural robustness and large specific surface area. These properties contribute to CNTs gaining extensive applications in the development of novel sensors [1,2]. Especially due to the remarkable electrocatalytic property and excellent electrical conductivity, CNTs are commonly applied to directly electrocatalyze interesting analytes including hydrogen [3], methanol [4,5], hydrogen peroxide [6–8], nitrite [9], phenols and vitamin B [10,11]. Most of these studies, however, modify the electrode substrates by simply drop-casting and immobilizing CNTs with physical adsorption, resulting in a random and chaotic arrangement of nanotubes and dramatically

reducing the active sites exposed. Hence, an interesting question is how to fabricate tailored architectures with CNTs and further improve their properties such as catalytic ability, electron transfer quality and mechanical stability. Since Smalley and coworkers [12] linked the acid-treated CNTs to alkanethiol by the amide linkage and then tethered the free thiol end to gold particles by the Au–S bond, this novel self-assembly method has been regarded as an efficient route to immobilize CNTs. Self-assembly can make CNTs well-organized on the electrode surface and provide more electron communication tunnels [13], and make electron transfer easier due to the high conductance of the edge plane of CNTs [1]. Furthermore, aligned CNTs are proven capable of facilitating the direct electron transfer between the redox-active enzymes and the electrode surface [14–16].

Meanwhile, tailored metal nanostructures have also been widely applied to fabricate novel sensors and devices due to their unique electronic, optical and catalytic properties [17]. As an excellent electrode material, nanostructured platinum is of particular interest for the development of electrochemical sensors and biosensors owing to its electrochemical stability and prominent catalytic activity [18]. There are many reports involved in utilizing platinum nanostructure-decorated carbon nanotubes randomly

\* Corresponding author at: Shanghai Key Laboratory of Functional Materials Chemistry, and Research Centre of Analysis and Test, East China University of Science and Technology, Shanghai 200237, PR China. Tel.: +86 21 64253574; fax: +86 21 64252947.

E-mail address: [minbolan@ecust.edu.cn](mailto:minbolan@ecust.edu.cn) (M. Lan).



Scheme 1

**Scheme 1.** Illustration of the fabrication of SPGFE/MWCNTC/PtNP.

adsorbed on the electrode surface to electrocatalyze interesting materials for sensing and fuel cell [19–23], while these chaotic structures reveal a number of disadvantages. The electron communication, for example, is partially restricted because of the limited transfer tunnels. More seriously, the adsorbed CNTs are easily exfoliated from the substrate, dramatically weakening their reliability, long-term stability and wider applications in practical sensing. Therefore, increasing attention has been focused on the highly ordered carbon nanotube/nanostructured material hybrid architectures and their applications in electrochemical sensing and fuel cell [24–27].

Here we introduce a multi-walled carbon nanotube cluster/platinum nanoparticle hybrid structure on a screen-printed gold nanofilm electrode (SPGFE/MWCNTC/PtNP) substrate for the electrocatalysis and determination of hydrogen peroxide. Covalent-linked multi-walled carbon nanotubes were vertically aligned on the screen-printed gold nanofilm electrode (SPGFE) surface and further formed carbon nanotube clusters (MWCNTC). Then platinum nanoparticles (PtNPs) were in situ synthesized by electrochemically reducing chloroplatinic acid with a cyclic voltammetric deposition on the MWCNTC structure. The electrocatalytic behavior of SPGFE/MWCNTC/PtNP toward hydrogen peroxide was intensively discussed. Several parameters affecting the electroanalytical performances of the proposed electrode were further optimized, and the sensitivity, reproducibility and selectivity of the fabricated non-enzymatic sensor for hydrogen peroxide detection were also evaluated.

## 2. Experimental

### 2.1. Materials and chemicals

Multi-walled carbon nanotubes (MWCNTs) with a mean diameter of 15 nm and a mean tube length of 1.5  $\mu\text{m}$  were provided by Shenzhen Nanotech Port Co.  $\beta$ -Mercaptoethylamine (MEA) and dicyclohexyl carbodiimide (DCC) were commercially available from Aladdin Chemistry Co. Hexachloroplatinic(IV) acid hexahydrate ( $\text{H}_2\text{PtCl}_6 \cdot 6\text{H}_2\text{O}$ , Sigma–Aldrich Co.) was diluted to 2 wt% as the platinum precursor. Hydrogen peroxide ( $\text{H}_2\text{O}_2$ , Sinopharm Chemical Reagent Co.) was stored under 4  $^\circ\text{C}$  and diluted before use. 0.1 M phosphate buffer solution (PBS, pH 6.9) prepared with  $\text{K}_2\text{HPO}_4$  and  $\text{KH}_2\text{PO}_4$  was used as the supporting electrolyte. All other reagents were of analytical grade and used without further purification. Ultra-pure water (18.2  $\text{M}\Omega\text{cm}$ ) prepared by a laboratory water purification system (Shanghai Hitech Instruments Co.) was utilized in all preparations.

### 2.2. Preparation of SPGFE

The procedure employed in the preparation of the SPGFE substrate has been described in our previous reports [28,29]. A gold thin film with a thickness of  $75 \pm 5\text{ nm}$  determined by atomic force microscope was obtained using the vacuum sputtering technique, with an evaporation time of 300 s and an excitation current of 40 mA, on a JEC-1600 fine vacuum evaporation instrument.

The diameter of the gold working area was determined to be 4 mm.

### 2.3. Immobilization of MWCNTC

Prior to immobilizing nanotubes onto the SPGFE mirror-like surface, MWCNTs were shortened and carboxyl functionalized using a similar procedure as described in [12,14,30]. Briefly, purified MWCNTs in a mixture (3:1, v/v) of  $\text{H}_2\text{SO}_4$  (98%) and  $\text{HNO}_3$  (70%) were treated with ultrasonic stimulation for 4 h, and then rinsed with adequate ultrapure water and dried overnight in the oven at  $50^\circ\text{C}$ . Afterwards, 1 mg of treated MWCNTs was well dispersed in 5 mL of ultrapure water with 2.5 mg of DCC to convert the carboxyl group at the ends of nanotubes into active carbodiimide esters [30]. Meanwhile, the SPGFE substrate was modified with an oriented MEA monolayer by incubating the clean SPGFE into a solution containing 1 mM MEA for 6 h. Finally, the MEA monolayer-modified electrode was incubated in the carbon nanotube solution for 8 h at room temperature, while the free amine at the terminal of MEA formed the amide bond with one end of the acid-treated MWCNTs. Scheme 1 illustrates the self-assembly steps of MWCNTs on the SPGFE substrate to prepare carbon nanotube clusters.

### 2.4. Decoration of MWCNTC with PtNPs

The modification of PtNPs onto the MWCNTC structure was in situ obtained by electrochemically reducing  $\text{H}_2\text{PtCl}_6$ . Briefly, the cyclic voltammetric (CV) technique with a potential window from +0.3 to +1.3 V was employed to prepare PtNPs in a chloroplatinic acid bath, followed by a cyclic scan procedure from  $-0.3$  to +1.0 V in 0.5 M  $\text{H}_2\text{SO}_4$  to a steady state [31,32].

### 2.5. Apparatus and measurements

All electrochemical experiments were carried out on a CHI 440A electrochemical station (CHI Instruments Inc.) with a conventional three-electrode configuration including a fabricated working electrode, a platinum wire counter electrode and a saturated Ag/AgCl reference electrode. All potentials in the present research were referred to the saturated Ag/AgCl electrode unless otherwise stated.

The prepared SPGFE/MWCNTC/PtNP was well characterized by several physical and chemical techniques. The atomic force microscopy (AFM) image was obtained with atomic force microscope (Nanoscope III Multimode, Veeco, USA). The surface morphology of electrodes was observed by field emission scanning electron microscope (S-4800 FESEM, Hitachi, Japan). The immobilization process of MWCNTC on the SPGFE substrate was also supported by cyclic voltammetric scanning from  $-0.5$  to +0.5 V in 0.1 M PBS solutions. The electrocatalytic behavior of SPGFE/MWCNTC/PtNP toward  $\text{H}_2\text{O}_2$  was intensively evaluated with the cyclic voltammetric and chronoamperometric techniques. All measurements were performed at room temperature ( $25 \pm 2^\circ\text{C}$ ).

## 3. Results and discussion

### 3.1. Characterization of SPGFE/MWCNTC/PtNP

In the present research, we introduced a new carbon nanotube cluster/noble metal hybrid nanostructure on the SPGFE substrate to electrocatalyze hydrogen peroxide. Several techniques were used to characterize the morphology and elemental component of the proposed structure. The AFM image of gold nanofilm electrodes (not shown) reveals that the as-prepared SPGFE has a flat and clean surface. Fig. 1(A) depicts the AFM image of MWCNTC on the

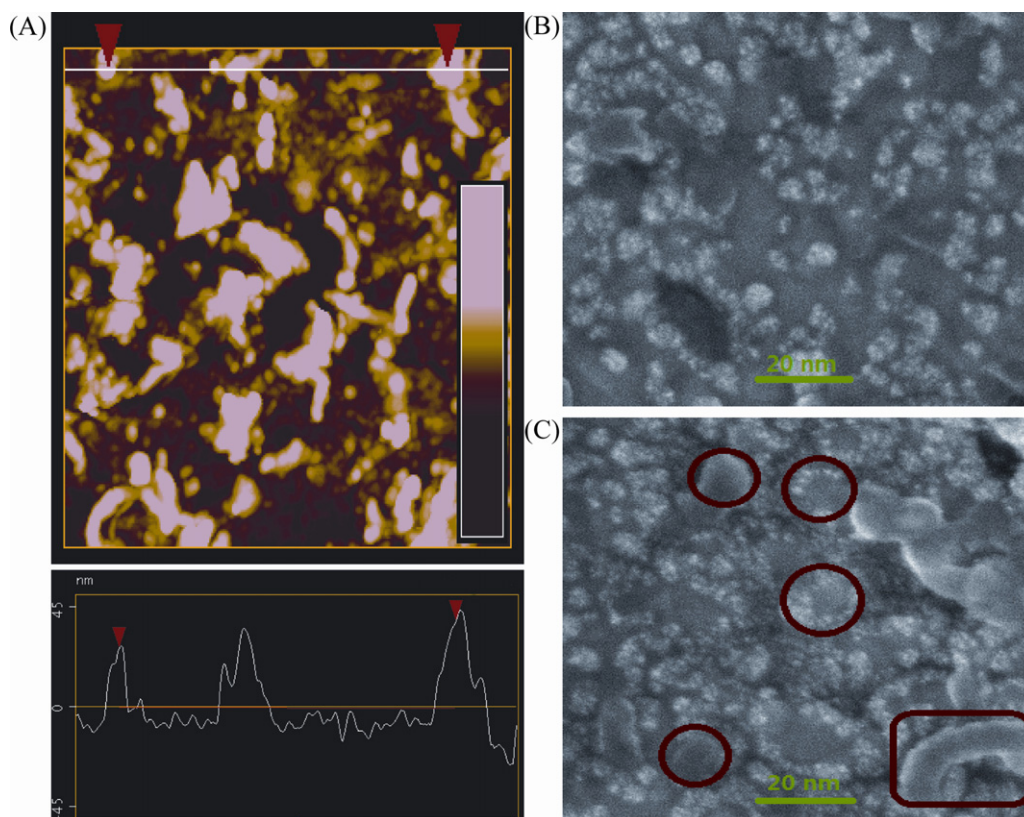
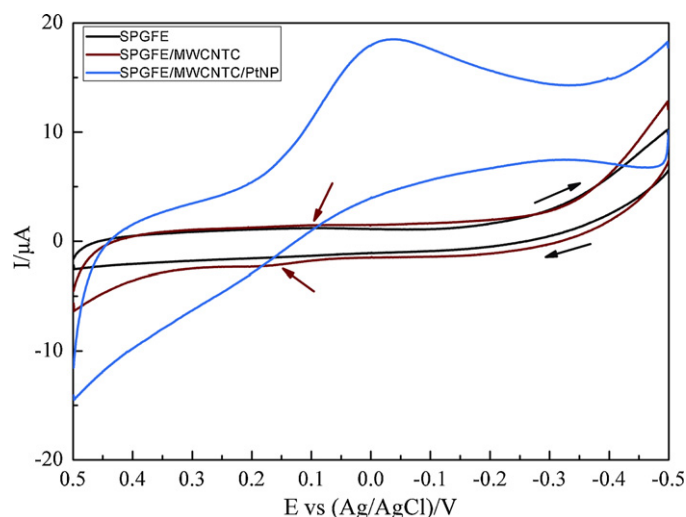


Fig. 1. AFM image of MWCNTC on the SPGFE surface (A), and SEM images of PtNPs on the SPGFE (B) and SPGFE/MWCNTC (C) surfaces.





**Fig. 2.** Cyclic voltammograms of the bare SPGFE, SPGFE/MWCNTC and SPGFE/MWCNTC/PtNP in 0.1 M PBS solutions (pH 6.9) at a scan rate of 100 mV/s with the potential window from  $-0.5$  to  $+0.5$  V.

SPGFE substrate. It is found that carbon nanotubes are vertically aligned on the electrode surface as expected, which is also demonstrated by Fig. S1 (Supporting Information). The height of carbon nanotubes is determined to be tens of nanometers, having a good agreement with previous reports [15,33]. The width of MWCNTC turns to be much larger than the diameter of a single MWCNT due to the aggregation of carbon nanotubes in the immobilization step [15]. Fig. 1(B) and (C) present the SEM patterns of PtNPs on the bare SPGFE and SPGFE/MWCNTC, respectively. As can be seen, PtNPs with a diameter of several nanometers are well dispersed on the SPGFE surface. When MWCNTC are formed on the SPGFE substrate, PtNPs are partially dispersed across the carbon nanotubes (Fig. 1(C)). This phenomenon may be explained as that the top ends and defects exposed can act as nucleus for the formation of platinum nanoparticles. It should be stated that there are also a few carbon nanotubes recumbently on the SPGFE surface. This phenomenon mainly results from that some carbon nanotubes are inevitably fixed by physical adsorption during the self-assembly process and cannot be completely rinsed off.

The self-assembly of CNTs on the SPGFE substrate and the electrodeposition preparation of platinum nanoparticles were also characterized by electrochemical techniques. Fig. 2 shows the typical cyclic voltammograms of the bare SPGFE, SPGFE/MWCNTC and SPGFE/MWCNTC/PtNP in 0.1 M PBS solutions at a scan rate of 100 mV/s. As we can see, the bare SPGFE exhibits no current response in the potential window from  $-0.5$  to  $+0.5$  V. When MWCNTs are immobilized on the SPGFE substrate by self-assembly and form nanotube cluster structures, a pair of weak but recognizable redox peaks are observed at around  $+0.15$  V, which should be assigned to the carboxylate in non-oriented carbon nanotubes [15,34]. After the electrochemical deposition procedure, PtNPs are in situ synthesized on the MWCNTC structure, which has been demonstrated by Fig. 1(B) and (C). As a result, a remarkable peak is obtained at  $+0.05$  V. This reduction current peak is attributed to the specific response of platinum oxide in PBS solutions, and correspondingly, a flat double layer region at potential more positive than  $+0.2$  V should be ascribed to the platinum oxide formation. The specific redox peaks of functionalized carbon nanotubes are not observed for SPGFE/MWCNTC/PtNP because they are totally covered by the amplified background signal. In addition, the hydrogen adsorption/desorption responses are observed at potentials more negative than  $-0.45$  V in 0.1 M PBS solutions. These proofs also confirm the successful fabrication of SPGFE/MWCNTC/PtNP.

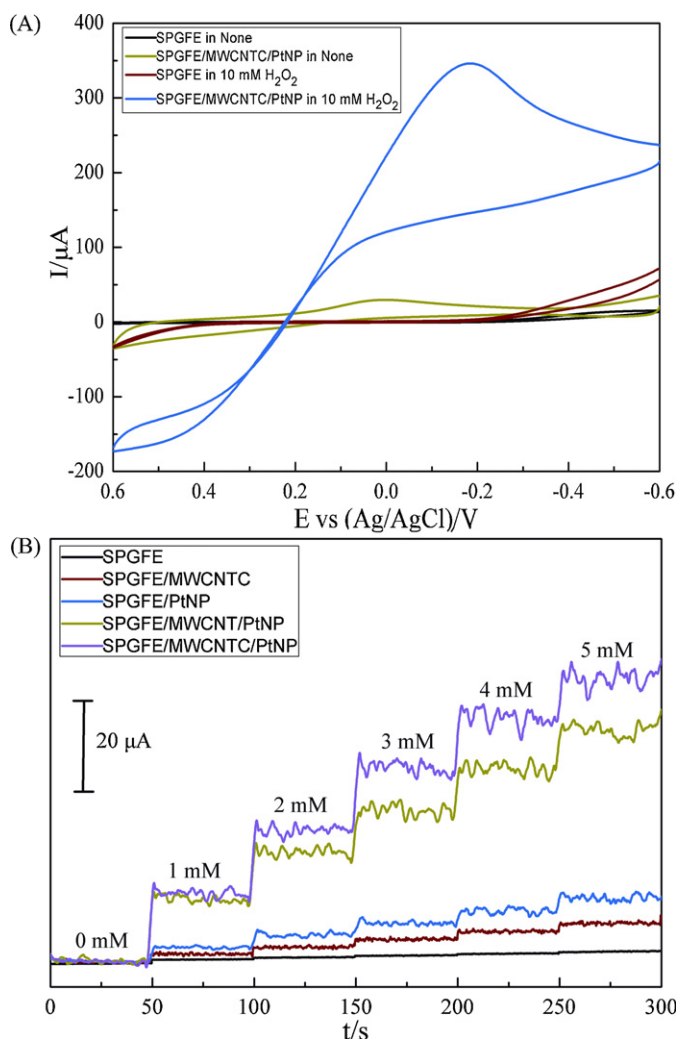


**Fig. 3.** (A) Cyclic voltammograms of the bare SPGFE and SPGFE/MWCNTC/PtNP in 0.1 M PBS solutions (pH 6.9) with the absence and presence of 10 mM H<sub>2</sub>O<sub>2</sub> at a scan rate of 100 mV/s, and (B) typical amperometric responses of the bare SPGFE, SPGFE/MWCNTC, SPGFE/PtNP, SPGFE/MWCNT/PtNP and SPGFE/MWCNTC/PtNP for different concentrations of H<sub>2</sub>O<sub>2</sub> in 0.1 M PBS solutions (pH 6.9) with an applied potential of  $-0.4$  V under a constant stir.

### 3.2. Electrocatalytic behavior of SPGFE/MWCNTC/PtNP toward H<sub>2</sub>O<sub>2</sub>

The electrocatalytic behavior of SPGFE/MWCNTC/PtNP toward H<sub>2</sub>O<sub>2</sub> was initially investigated with cyclic voltammetry. Fig. 3(A) depicts the typical cyclic voltammograms of the bare SPGFE and SPGFE/MWCNTC/PtNP in the absence and presence of 10 mM H<sub>2</sub>O<sub>2</sub>. Low background noises are observed on both electrodes in 0.1 M PBS solutions without H<sub>2</sub>O<sub>2</sub>. The current peak at around 0 V for SPGFE/MWCNTC/PtNP is assigned to the specific response of platinum nanoparticles in PBS solutions, which has been demonstrated by Fig. 2. When 10 mM H<sub>2</sub>O<sub>2</sub> is added, the bare SPGFE still exhibits no identifiable current response, while the SPGFE/MWCNTC/PtNP provides a remarkable reduction signal of H<sub>2</sub>O<sub>2</sub> at  $-0.2$  V. It reveals that the proposed SPGFE/MWCNTC/PtNP can significantly enhance the electrocatalytic reduction of H<sub>2</sub>O<sub>2</sub> in neutral solutions.

To further confirm the prominent electrocatalytic performances of the proposed SPGFE/MWCNTC/PtNP, the fabricated electrode as well as electrodes modified with only MWCNTC (SPGFE/MWCNTC) or PtNPs (SPGFE/PtNP) was used to monitor hydrogen peroxide with the chronoamperometric technique. For comparison, the electrocatalytic performances of platinum

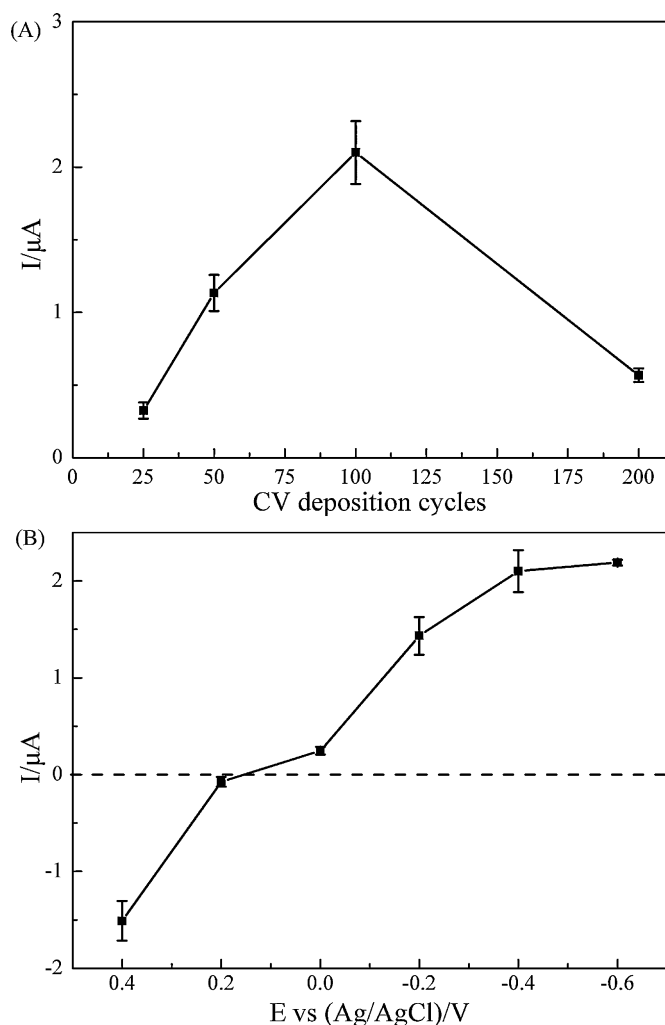


**Fig. 4.** (A) Effects of the CV deposition cycle on the reduction current of 0.1 mM  $\text{H}_2\text{O}_2$  at  $-0.4$  V, and (B) effects of the applied potential on the amperometric response of 0.1 mM  $\text{H}_2\text{O}_2$  under a constant stir.

nanoparticle-loaded MWCNTs randomly adsorbed on the SPGFE substrate (SPGFE/MWCNT/PtNP) by use of the common drop-casting method for  $\text{H}_2\text{O}_2$  were also recorded. Fig. 3(B) shows the typical amperometric responses of different modified electrodes measured at a potential of  $-0.4$  V in 0.1 M PBS solutions with successive additions of  $\text{H}_2\text{O}_2$ . At this potential, these electrodes will not provide the specific signal of platinum, and the attributions from hydrogen adsorption/desorption responses are also very limited. In comparison with the bare SPGFE, both SPGFE/MWCNTC and SPGFE/PtNP can greatly enhance the electrocatalytic reduction of  $\text{H}_2\text{O}_2$ . As shown in Fig. 3(B), when the carbon nanotube/platinum hybrid structures (MWCNT/PtNP and MWCNTC/PtNP) are introduced on the SPGFE substrate, both electrodes (SPGFE/MWCNT/PtNP and SPGFE/MWCNTC/PtNP) turn to be more sensitive toward additions of  $\text{H}_2\text{O}_2$ . Encouragingly, among these modified electrodes, the proposed SPGFE/MWCNTC/PtNP presents the most sensitive responses, especially for high concentration  $\text{H}_2\text{O}_2$ . It is initially considered that this phenomenon mainly attributes to the property that carbon nanotubes vertically aligned on the electrode surface can offer more active sites and surface areas for the loading of PtNPs [24]. Besides, chemically immobilized carbon nanotubes can play a role of the electron bridge connecting the electrode body with the analytes, providing more electron communication tunnels and making electron transfer faster due to the high conductance of the edge plane [1,13,17]. The efficient

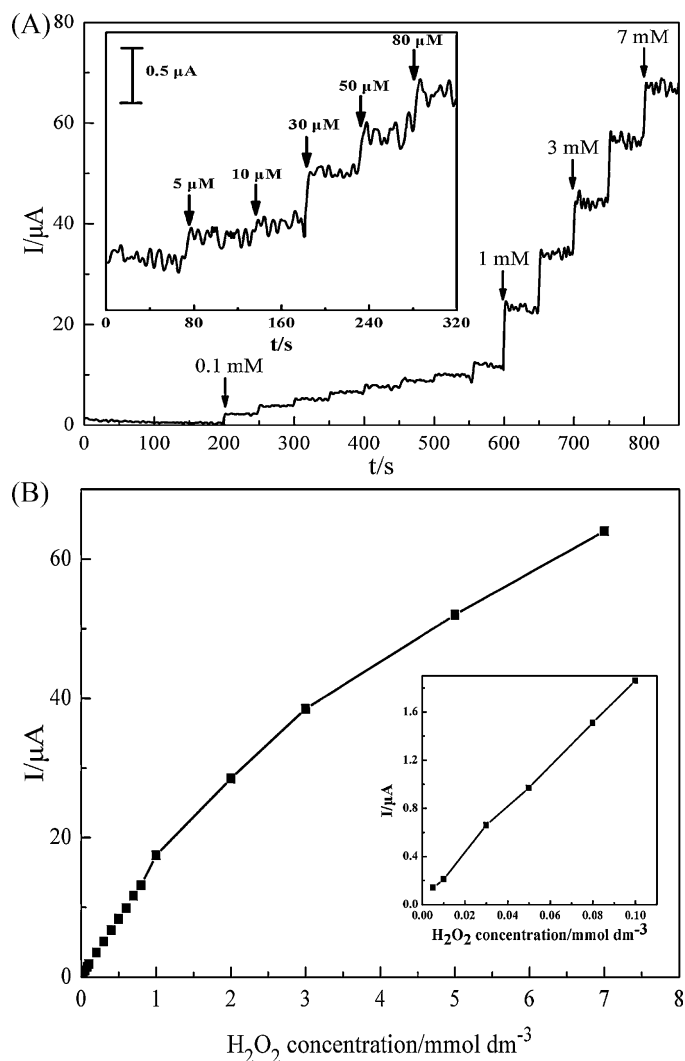


**Fig. 5.** (A) Typical amperometric responses for successive additions of  $\text{H}_2\text{O}_2$  in 0.1 M PBS solutions (pH 6.9) at SPGFE/MWCNTC/PtNP with an applied potential of  $-0.4$  V under a constant stir, and (B) plots of the reduction currents vs the concentrations of  $\text{H}_2\text{O}_2$ .

contact between platinum nanoparticles and the top ends of carbon nanotubes, as shown in Fig. 1(C), greatly facilitates the electron transfer.

### 3.3. Parameter optimization

Prior to quantitative measurements of  $\text{H}_2\text{O}_2$ , several experimental parameters affecting the detecting system were further optimized. Fig. 4(A) depicts the effect of the CV deposition cycle which determines the quantity and size of PtNPs on the reduction current of 0.1 mM  $\text{H}_2\text{O}_2$ . The current response increases correspondingly with the deposition cycle number expanding to one hundred cycles. When a deposition cycle of two hundred is selected, the current response of  $\text{H}_2\text{O}_2$  exhibits a sharp decrease. It is roughly considered that too long deposition time may result in the agglomeration of PtNPs and reduce the electrocatalytic ability of PtNPs [31]. Therefore, a CV deposition of one hundred cycles is employed to prepare PtNPs in the following research.

Fig. 4(B) shows the influence of the applied potential on the amperometric response of 0.1 mM  $\text{H}_2\text{O}_2$ . When  $+0.4$  V is used, an oxidation response is observed. At potentials more negative than  $+0.15$  V,  $\text{H}_2\text{O}_2$  is electrochemically reduced in neutral solutions, and the current signal increases accordingly with the applied potential

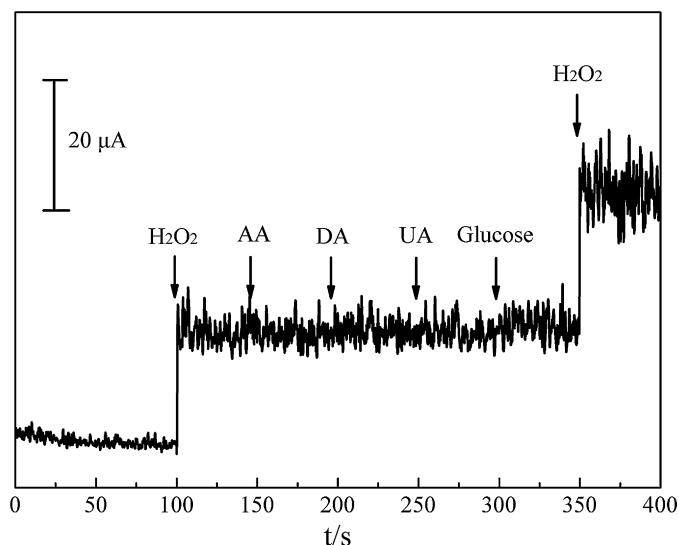


**Fig. 6.** Typical amperometric responses of 1 mM  $\text{H}_2\text{O}_2$ , ascorbic acid (AA), dopamine (DA), uric acid (UA) and glucose in 0.1 M PBS solutions (pH 6.9) at SPGFE/MWCNTC/PtNP with an applied potential of  $-0.4\text{ V}$  under a constant stir.

negatively shifting to  $-0.6\text{ V}$ . With consideration of the interferences from other physiological materials, the applied potential of  $-0.4\text{ V}$  is regarded as an appropriate compromise between sensitivity and selectivity.

### 3.4. Electroanalytical performances

Quantitative amperometric measurements of  $\text{H}_2\text{O}_2$  were carried out under the above optimum conditions. Fig. 5(A) presents the typical amperometric responses for successive additions of  $\text{H}_2\text{O}_2$  at the proposed SPGFE/MWCNTC/PtNP. The reduction currents, as shown in Fig. 5(B), linearly increase with  $\text{H}_2\text{O}_2$  concentrations in the scope from 5 to  $2000\text{ }\mu\text{M}$  with a correlation coefficient of 0.9912. As for higher concentration  $\text{H}_2\text{O}_2$ , the proposed electrode slightly suffers from the common saturation effect. The limit of detection is calculated to be as low as  $1.23\text{ }\mu\text{M}$ , which is comparable or even lower to that of modified silver paste electrodes [35] and nanoporous gold electrodes [36]. Such excellent performances can be attributed to the outstanding electrocatalytic activity of nanostructured platinum and aligned CNTs and their beneficial synergistic effect. It should be mentioned that aligned carbon nanotubes without uniform lengths may amplify the background noise and restrict the detection limit. Hence, future work is worthy to reduce the background noise.

Good reproducibility is another attractive feature of the proposed SPGFE/MWCNTC/PtNP. Measurements of 1 mM  $\text{H}_2\text{O}_2$  at eight prepared electrodes lead to repeatable results with a relative standard deviation (RSD) of 6.9%. In order to investigate the selectivity of the non-enzymatic sensor, the possible interferences from several physiological materials including ascorbic acid (AA), dopamine (DA), uric acid (UA) and glucose were assessed. As shown in Fig. 6, it is found that there is no distinct influence from additions of 1 mM AA, DA, UA and glucose upon the detection of  $\text{H}_2\text{O}_2$  (1 mM), indicating that the fabricated non-enzymatic electrode can be applied for the selective detection of  $\text{H}_2\text{O}_2$  in the presence of these common physiological materials.

## 4. Conclusions

We demonstrated that the novel MWCNTC/PtNP hybrid structure on the SPGFE substrate could significantly enhance the electrocatalytic reduction of  $\text{H}_2\text{O}_2$  in neutral oxygen-containing

solutions. The fabricated non-enzymatic sensor exhibited high sensitivity, good reproducibility and excellent selectivity for  $\text{H}_2\text{O}_2$  determination. The results also revealed that the proposed PtNP-modified carbon nanotube clusters vertically aligned on the SPGFE surface could provide preferable electrocatalysis performances for  $\text{H}_2\text{O}_2$  reduction than the common PtNP-modified CNTs. The proposed carbon nanotube cluster/metal hybrid nanostructure is expected to be a promising candidate as a scaffold for the fabrication of biosensors.

## Supporting information

Supporting information contains the AFM pattern of MWCNTC immobilized on the SPGFE substrate by self-assembly.

## Acknowledgments

This work was financially supported by Science and Technology Commission of Shanghai Municipality (STCSM, Contract No. 10dz2220500 and No. 10391901600) and Ministry of Education of the People's Republic of China (Contract No. WK1014051).

## Appendix A. Supplementary data

Supplementary data associated with this article can be found, in the online version, at doi:10.1016/j.electacta.2012.01.030.

## References

- [1] J. Wang, Y.-H. Lin, *Trends Anal. Chem.* 27 (2008) 619.
- [2] D. Vairavapandian, P. Vichchulada, M.D. Lay, *Anal. Chim. Acta* 626 (2008) 119.
- [3] D.-D. La, C.-K. Kim, T.-S. Jun, Y. Jung, G.-H. Seong, J. Choo, Y.-S. Kim, *Sens. Actuators B* 155 (2011) 191.
- [4] K. Lee, J.-W. Lee, S. Kim, B.-K. Ju, *Carbon* 49 (2011) 787.
- [5] K.M. Samant, V.S. Joshi, G. Sharma, S. Kapoor, S.K. Haram, *Electrochim. Acta* 56 (2011) 2081.
- [6] A. Salimi, M. Mandioun, A. Noorbakhsh, A. Abdolmaleki, R. Ghavami, *Electrochim. Acta* 56 (2011) 3387.
- [7] Y. Shi, Z.-L. Liu, B. Zhao, Y.-J. Sun, F.-G. Xu, Y. Zhang, Z.-W. Wen, H.-B. Yang, Z. Li, *J. Electroanal. Chem.* 656 (2011) 29.
- [8] M.-Y. Hua, H.-C. Chen, R.-Y. Tsai, S.-J. Tseng, S.-C. Hu, C.-D. Chiang, P.-J. Chang, *J. Phys. Chem. C* 115 (2011) 15182.
- [9] G.L. Turdean, I.C. Popescu, A. Curulli, G. Palleschi, *Electrochim. Acta* 51 (2006) 6435.
- [10] Y. Umasankar, A.P. Periasamy, S.-M. Chen, *Anal. Biochem.* 411 (2011) 71.
- [11] Y. Umasankar, T.-W. Ting, S.-M. Chen, *J. Electrochem. Soc.* 158 (2011) 117.
- [12] J. Liu, A.G. Rinzier, H. Dai, J.H. Hafner, R.K. Bradley, P.J. Boul, A. Lu, T. Iverson, K. Shelimov, C.B. Huffman, F. Rodriguez-Macias, Y.-S. Shon, T.R. Lee, D.T. Colbert, R.E. Smalley, *Science* 280 (1998) 1253.
- [13] D. Chattopadhyay, I. Galeska, F. Papadimitrakopoulos, *J. Am. Chem. Soc.* 123 (2001) 9451.
- [14] J.J. Gooding, R. Wibowo, J.-Q. Liu, W.-R. Yang, D. Losic, S. Orbons, F.J. Mearns, J.G. Shapter, D.B. Hibbert, *J. Am. Chem. Soc.* 125 (2003) 9006.
- [15] X. Yu, D. Chattopadhyay, I. Galeska, F. Papadimitrakopoulos, J.F. Rusling, *Electrochem. Commun.* 5 (2003) 408.
- [16] F. Patolsky, Y. Weizmann, I. Willner, *Angew. Chem. Int. Ed.* 43 (2004) 2113.
- [17] I. Willner, B. Willner, *Nano Lett.* 10 (2010) 3805.
- [18] O.A. Sadik, A.O. Aluoch, A.-L. Zhou, *Biosens. Bioelectron.* 24 (2009) 2749.
- [19] M.-C. Tsai, T.-K. Yeh, C.-H. Tsai, *Int. J. Hydrogen Energy* 36 (2011) 8261.
- [20] O.Y. Ivashina, M.E. Tamm, E.V. Gerasimova, M.P. Kochugaeva, M.N. Kirikova, S.V. Savilov, L.V. Yashina, *Inorg. Mater.* 47 (2011) 618.
- [21] D.-P. He, C. Zeng, C. Xu, N.-C. Cheng, H.-G. Li, S.-C. Mu, M. Pan, *Langmuir* 27 (2011) 5582.
- [22] O. Winjobi, Z.-Y. Zhang, C.-H. Liang, W.-Z. Li, *Electrochim. Acta* 55 (2011) 4217.
- [23] Z.-P. Guo, D.-M. Han, D. Wexler, R. Zeng, H.-K. Liu, *Electrochim. Acta* 53 (2008) 6410.
- [24] B.-H. Wu, Y.-J. Kuang, X.-H. Zhang, J.-H. Chen, *Nano Today* 6 (2011) 75.
- [25] H. Chen, A. Roy, J.-B. Baek, L. Zhu, J. Qu, L.-M. Dai, *Mater. Sci. Eng. Rep.* 70 (2010) 63.
- [26] Y.-J. Kuang, B.-H. Wu, Y. Cui, Y.-M. Yu, X.-H. Zhang, J.-H. Chen, *Electrochim. Acta* 56 (2011) 8645.
- [27] A. Zloczewska, M. Jönsson-Niedziolka, J. Rogalski, M. Opallo, *Electrochim. Acta* 56 (2011) 3947.
- [28] X.-H. Niu, Y.-L. Ding, C. Chen, H.-L. Zhao, M.-B. Lan, *Sens. Actuators B* 158 (2011) 383.

- [29] Y.-J. Teng, X.-B. Wu, Q. Zhou, C. Chen, H.-L. Zhao, M.-B. Lan, *Sens. Actuators B* 142 (2009) 267.
- [30] Z.-F. Liu, Z.-Y. Shen, T. Zhu, S.-F. Hou, L.-Z. Ying, Z.-J. Shi, Z.-N. Gu, *Langmuir* 16 (2000) 3569.
- [31] Y. Zhao, L.-Z. Fan, H.-Z. Zhong, Y.-F. Li, S.-H. Yang, *Adv. Funct. Mater.* 17 (2007) 1537.
- [32] D.-J. Guo, H.-L. Li, *J. Electroanal. Chem.* 573 (2004) 197.
- [33] P. Diao, Z.-F. Liu, B. Wu, X.-L. Nan, J. Zhang, Z. Wei, *ChemPhysChem* 3 (2002) 898.
- [34] H.-X. Luo, Z.-J. Shi, N.-Q. Li, Z.-N. Gu, Q.-K. Zhuang, *Anal. Chem.* 73 (2001) 915.
- [35] L. Gonzalez-Macia, M.R. Smyth, A. Morrin, A.J. Killard, *Electrochim. Acta* 56 (2011) 4146.
- [36] F.-H. Meng, X.-L. Yan, J.-G. Liu, J. Gu, Z.-G. Zou, *Electrochim. Acta* 56 (2011) 4657.